CrossMark

The Arabidopsis chloroplast RNase J displays both exo- and robust endonucleolytic activities

Michal Halpert[1] · Varda Liveanu[1] · Fabian Glaser[1,2] · Gadi Schuster[1]

Abstract

Key message **Arabidopsis chloroplast RNase J displaces both exo- and endo-ribonucleolytic activities and contains a unique GT-1 DNA binding domain.**

Abstract Control of chloroplast gene expression is predominantly at the post-transcriptional level via the coordinated action of nuclear encoded ribonucleases and RNA-binding proteins. The 5′ end maturation of mRNAs ascribed to the combined action of 5′→3′ exoribonuclease and gene-specific RNA-binding proteins of the pentatricopeptide repeat family and others that impede the progression of this nuclease. The exo- and endoribonuclease RNase J, the only prokaryotic 5′→3′ ribonuclease that is commonly present in bacteria, Archaea, as well as in the chloroplasts of higher plants and green algae, has been implicated in this process. Interestingly, in addition to the metalo-β-lactamase and β-CASP domains, RNase J of plants contains a conserved GT-1 domain that was previously characterized in transcription factors that function in light and stress responding genes. Here, we show that the Arabidopsis RNase J (*At*RNase J), when analyzed in vitro with synthetic RNAs, displays both 5′→3′ exonucleolytic activity, as well as robust endonucleolytic activity as compared to its bacterial homolog RNase J1 of *Bacillus subtilis*. *At*RNase J degraded single-stranded RNA and DNA molecules but displays limited activity on double stranded RNA. The addition of three guanosines at the 5′ end of the substrate significantly inhibited the degradation activity, indicating that the sequence and structure of the RNA substrate modulate the ribonucleolytic activity. Mutation of three amino acid in the catalytic reaction center significantly inhibited both the endonucleolytic and exonucleolytic degradation activities, while deletion of the carboxyl GT-1 domain that is unique to the plant RNAse J proteins, had a little or no significant effect. The robust endonucleolytic activity of *At*RNase J suggests its involvement in the processing and degradation of RNA in the chloroplast.

Keywords RNA-processing in the chloroplast · Metallo-beta-lactamase ribonuclease · GT-1 domain · 5′ to 3′ exoribonuclease

✉ Gadi Schuster
Gadis@technion.ac.il

1 Faculty of Biology, Technion—Israel Institute of Technology, 32000 Haifa, Israel

2 Bioinformatics Knowledge Unit, The Lorry I. Lokey Interdisciplinary Center for Life Sciences and Engineering, Technion—Israel Institute of Technology, 32000 Haifa, Israel

Introduction

Chloroplasts and mitochondria are endosymbionts, i.e., once free-living prokaryotes which have adapted over millions of years to life in the eukaryotic cell. These organelles feature a quixotic blend of ancestral and acquired characters, as is readily revealed in their RNA metabolism. Among the ancestral features are conserved ribonucleases such as RNases E and J, RNase II/R and polynucleotide phosphorylase (PNPase), as well as a polyadenylation-assisted RNA degradation pathway (Stern et al. 2010). At the same time, plant organelles also employ hundreds of helical repeat proteins to regulate various facets of their gene expression, such as RNA stability, splicing and editing (Barkan and Small 2014; Manavski et al. 2018). RNA ends are defined by

sequence-specific binding proteins, including the pentatrico-peptide repeat (PPR), tetratricopeptide repeat (TPR) proteins and several other groups (Barkan 2011; Prikryl et al. 2011; Zhelyazkova et al. 2012), as well as secondary structures. RNase J is postulated to be responsible for the generation of the 5′ end of the transcript by 5′→3′ digesting the precursor RNA until inhibited by the barrier formed by the transcript specific RNA binding protein, mostly of the PPR family, bound to its RNA-binding site.

RNase J1 (and the related J2) were first described in *B. subtilis* (Even et al. 2005). RNase J homologs are present in most bacteria, Archaea, chloroplasts and eukaryotic cells, suggesting that it is a general ancient ribonuclease that appeared relatively early in evolution (Condon and Gilet 2011; Dominski et al. 2013; Phung et al. 2013; Clouet-d'Orval et al. 2018). Its ancestral position can be exempli-fied by the methanogenic Archaea *Methanocaldococcus jannaschii*, where four RNase J and CPSF (cleavage and polyadenylation specific factor) homologs were character-ized, but no other genes encoding known ribonucleases are present (Levy et al. 2011). RNase J contains a metallo-β-lactamase domain (MBL), usually followed by β-CASP and RNA recognition (RRM) domains found in other RNA metabolism factors (Fig. 1), is active as a dimer or tetramer and hydrolyses RNA in a catalytic mechanism, in which a water molecule is coordinated by two zinc ions and is activated to be a hydroxyl ion so as to achieve an in-line nucleophilic attack for hydrolytic cleavage (Pei et al. 2015; Zheng et al. 2017). RNase J of plants are longer than their homologs from bacteria and Archaea and contain a C-termi-nal region that displays high homology to the GT-1 DNA-binding domain (Sharwood et al. 2011). Remarkably, most RNase J members have a combination of 5′→3′ exonuclease activity and endonuclease activity, that has been predicted based on the crystal structure of the bacterial and archaeal enzymes (De La Sierra-Gallay et al. 2008; Condon and Gilet 2011; Dorleans et al. 2011; Pei et al. 2015; Zheng et al. 2017). Its most studied homolog in human, CPSF73 (cleav-age and polyadenylation specific factor 73), is responsible for the cleavage of precursor mRNAs prior to addition of the stabilizing 3′ poly(A)-tail. In addition, CPSF73 functions in the processing of histone mRNAs and displays both exo- and endoribonuclease activities as a recombinant protein (Dominski et al. 2013). Only three RNase J members were reported so far to exhibit exclusively endonucleolytic activ-ity when tested in vitro. These are RNase J2 of the methano-genic Archaea *Methanocaldococcus jannaschii*, RNase J2 of *Bacillus subtilis* and RNase J of *Chlamydomonas reinhardtii* chloroplast (Condon and Gilet 2011; Levy et al. 2011; Liponska et al. 2018). In addition, the human β-lactamase short protein, LACTB2, that is active in the mitochondria, exclusively displaces endoribonucleolytic activity in vitro (Levy et al. 2016).

Chloroplasts of higher plants possess both RNases E and J, as do cyanobacteria, while *Chlamydomonas* contains RNase J but not RNase E. Previous evidence of 5′→3′ exo-ribonuclease activity in the 5′ end processing of chloroplast transcripts in *Chlamydomonas* is likely be the result of RNase J activity (Drager et al. 1998, 1999). Whether RNase J is an essential enzyme in *Chlamydomonas* is unknown. The only plants in which a mutant phenotype was studied are tobacco and Arabidopsis, where in the latter, a T-DNA insertion into the *RNJ* locus prevented embryo development (Tzafrir et al. 2004; Chen et al. 2015). To reveal changes in chloroplast RNA metabolism under conditions of RNase J deficiency, virus-induced gene silencing (VIGS) was used (Sharwood et al. 2011). The most striking effect was mas-sive accumulation of chloroplast antisense RNAs (asRNA), suggesting that failure of chloroplast RNA polymerase to terminate effectively leads to symmetric transcription prod-ucts that are normally eliminated by RNase J. If not elimi-nated by degradation, these antisense RNAs form duplexes with sense strand transcripts and prevent their translation. Therefore, in addition to its function in processing transcript 5′ ends (Stern et al. 2010; Barkan 2011; Prikryl et al. 2011; Zhelyazkova et al. 2012; Luro et al. 2013; Barkan and Small 2014; Manavski et al. 2018), RNase J plays a major role in RNA surveillance (Sharwood et al. 2011).

In this work, we describe the characterization of the ribo-nucleolytic activity of the Arabidopsis chloroplast RNase J in vitro. To this end, the protein was overexpressed in high quantity in yeast. We found that unlike its *Chlamydomonas* chloroplast homolog, Arabidopsis RNase J acts mainly on single-stranded RNA and DNA both as an exonuclease and as a robust endonuclease and that its mode of activ-ity is modulated by the sequence and structure of the RNA substrate.

Results

RNase J and the metallo-β-lactamase protein family

Figure 1a displays the domain structure of Arabidopsis RNase J (*AtRNase J*), which includes metallo-β-lactamase, β-CASP and RRM core domains, including the mostly con-served amino acids and motifs, and a GT-1 domain (Domin-ski 2007; Condon and Gilet 2011; Kaplan-Levy et al. 2012; Dominski et al. 2013). The GT-1 domain, which was defined in a family of about 30 transcription factors in Arabidopsis that activate mostly light-induced genes, is unique to RNase J of plants. It contains three helixes with each contains a conserved tryptophan, as well as an additional fourth amphi-pathic helix (Figs. 1b, S1, S2) (Kaplan-Levy et al. 2012). Interestingly, RNase J of *Chlamydomonas reinhardtii* is also long but lacks the GT-1 domain (Fig. 1a) (Liponska
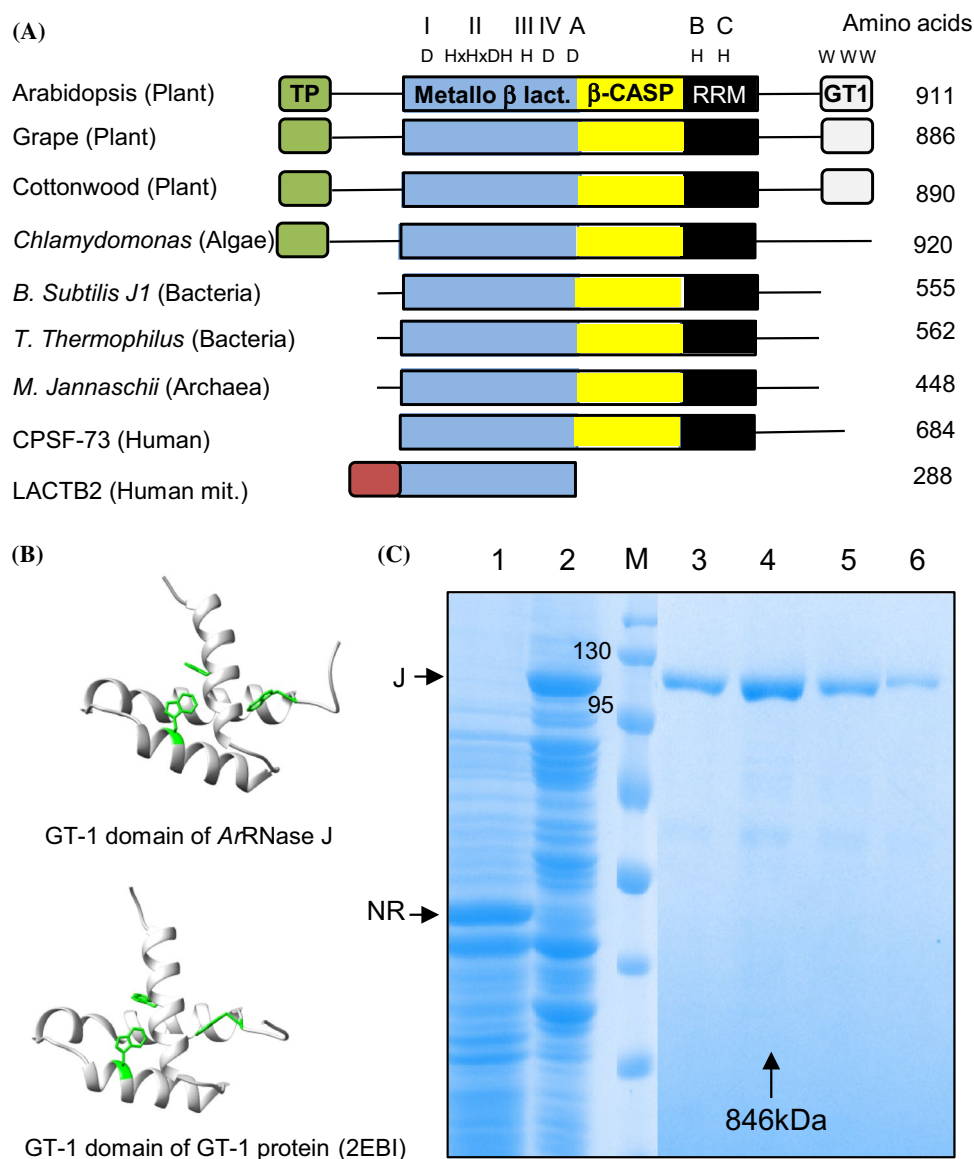
Fig. 1 Domain comparison of several plant, bacterial, archaeal and human β-CASP metallo-β-lactamase proteins, structural homology of the GT-1 domain and expression of the *At*RNase J in *P. pastoris*. **a** *Arabidopsis* RNase J (At5g63420) was used as a query to find homologous proteins. The domains of grape (*Vitis vinifera*; XM_002279762.1) and cottonwood (*Populus trichocarpa*; XM_002318086.1) plants, of *Chlamydomonas*, the bacteria *B. subtilis* (Q45493) and *T. thermophilus* (A0525) and of the archaea *Methanocaldococcus jannaschii* (Q58271), as well as of the human CPSF-73 and the mitochondrial protein LACTB2, are presented. The conserved motifs of the metallo-β-lactamase, β-CASP and RNA-recognition motive (RRM) (I–IV; A–C) are indicated in blue, yellow and black, respectively, along with the related amino acid residues. The predicted chloroplast transit peptide (TP) in the plant proteins and the mitochondrial TP in human LACTB2, are indicated in green and red, respectively. The plant C-terminal regions include a region homologous to the GT-1 DNA-binding domain (light gray). **b** Structural model of the GT-1 domain of *At*RNase J (upper), built using the NMR solved structure of the GT-1 transcription factor (2EBI, lower) (Nagata et al. 2010) as its template. The three conserved tryptophans are presented with stick model and green color. See further details in Fig. S1. **c** Coomassie-stained polyacrylamide gel of recombinant *At*RNase J (J) purified from *Pichia pastoris*. Lane 1, total proteins from cells expressing an unrelated protein (acetyl-coenzyme A acyl-transferase 2). Lane 2, total proteins from a strain expressing *At*RNase J; Lanes 3–6, eluted fractions from the Superdex 200 size-exclusion column. *M* molecular weight size markers. *At*RNase J was eluted following expression in *Pichia pastoris* as an RNA–protein complex of 846 kDa. Its identity was verified by immunoblotting using polyclonal anti-*At*RNase J or anti-His antibodies

et al. 2018). Plant and *Chlamydomonas* RNase J proteins contain a transit peptide sequence at their N-terminus, which direct these nuclear-encoded proteins to the chloroplast.

The human short endoribonuclease LACTB2 harbors a mitochondrial targeting sequence (Levy et al. 2016). The β-CASP and the RNA-recognition (RRM) domains of the

metallo-β-lactamase (MBL) are highly conserved and contain the several motifs that participate in the coordination of the two catalytic Zn^{2+} ions and the 5′ end phosphate binding site.

To explore the fold organization of the GT-1 domain of *At*RNase J, we structurally superimposed the structure of a MYB-like domain of the plant telomere binding protein, NgTRF, in complex with telomeric DNA (PDB 2QHB (HTH (helix turn helix) myb-type)) (Cho et al. 2008), with the structural model of the GT-1 domain of *At*RNase J (Nagano 2000; Kaplan-Levy et al. 2012; Qin et al. 2014). Although these peptides share only 12% sequence identity, their structures display high similarity, with a significant RMSD (root mean square deviation) (Meng et al. 2006) of ~ 4.0 Å between Cα atoms, suggesting a similar fold organization of the GT-1 typical three helixes motif (Figs. 1, S1). Most importantly, the location of the putative DNA–protein interface of the GT-1 domain of *At*RNase J, inferred by evolutionary and electrostatics data analysis in the model, is predicted to be located roughly on the same area as in the MYB-like domain structure, determined experimentally (Nagata et al. 2010). Taken together, these results suggest that the GT-1 domain of *At*RNase J encompasses a conserved putative DNA binding site which shares a similar physico-chemical characteristics and fold organization as in MYB-like GT-1 domain.

In our previous work, we developed a recombinant protein expression approach in bacteria, that enabled large-scale structure–function analysis of the plant RNase J (Sharwood et al. 2011). Considerable time was spent in attempts to optimize expression of the *At*RNase J in bacteria, by using multiple vectors and bacterial mutant backgrounds, e.g., lacking expression of typically contaminating RNases. Using this approach we were able to analyze the activity of the purified bacterially expressed *At*RNase J that displayed both an exo- and endoribonucleolytic activities (Sharwood et al. 2011). As we further pursued characterization of the enzyme, we turned to the yeast expression system. The absence of PNPase and RNase E proteins in this organism, favored production of large amounts of soluble recombinant protein devoid of any contaminating ribonucleolytic activity (Fig. 1c).

Robust endonucleolytic activity of Arabidopsis RNase J

When the purified enzyme was incubated with a 37-nt, AU-rich RNA, labeled at either the 5′ or 3′ end, distinct cleavage sites were obtained with the predominant one located at the middle of the molecule, 19 nt from the 5′ end (Fig. 2). The substrate RNA is 37 and 38-nt long when 5′ or 3′ labeled, respectively, due to the addition of C when labeling the 3′ end with pCp. Therefore, the major cleavage product with the length of 19 nt in both 5′ and 3′ labeled 37-nt substrate represents an endonucleolytic cleavage located 19 nt from the 5′ end (Fig. 2). In addition, since cleavage products were detected when the RNA was labeled at either the 5′ or the 3′ end, and since the major product was detected with both labeling methods, we concluded that these products resulted from endonucleolytic cleavages and not from stalling of an exonucleolytic activity. Yet, in addition to the endoribonucleolytic activity, [^{32}P]-AMP accumulated when the 5′ labeled substrate was used, reflecting 5′→3′ exonucleolytic activity. Since *At*RNase J displayed strong endonucleolytic activity, given the predominance of exonucleolytic activity of bacterial RNase J analyzed in vitro (Mathy et al. 2007), we compared it to that of the well-characterized *B. subtilis* RNase J1. Figure 2a shows that the bacterial enzyme degraded the substrate as an exonuclease, leaving no detectable endonucleolytic cleavage products, confirming our previous results with bacterially-expressed *At*RNase J, which displayed robust endonucleolytic activity as compared to its *Bacillus* homologue (Sharwood et al. 2011).

In order to locate the catalytic active site and to firmly ascertain that the observed activity was that of recombinant *At*RNase J and not a contaminant, the three key amino acids of motif II of the MBL domain were mutated. Motif II binds the zinc ions that are essential for catalytic activity and thus this recombinant version was expected to be inactive (De La Sierra-Gallay et al. 2008; Dorleans et al. 2011; Pei et al. 2015; Zheng et al. 2017). Accordingly, a double mutation in this domain (D78K and H79A) impaired both activities of *B. subtilis* RNase J1 and J2, as well as the archaeal protein (De La Sierra-Gallay et al. 2008; Zheng et al. 2017). When considering the relatively robust endo- activity of *At*RNase J, it was important to analyze the effect of similar mutations on the two types of ribonucleolytic activities. To do so, we replaced the three central amino acids of motif II, changing two histidines to alanines and aspartic acid to lysine (Fig. 2b). The mutated protein, termed Motif II, was expressed and purified as described for the wild type protein and then incubated with the 5′ labeled 37 nt RNA. The degradation rate of Motif II mutated protein was significantly compromised; while the wild type protein degraded about 60% of the full length substrate in 90 min of incubation, no decrease in the initial amount of the substrate was observed with the Motif II mutant (Fig. 2). No accumulation of the corresponding degradation products was detected, indicating that both endo- and exo- activities were impaired. Therefore, as in *B. subtilis*, both the exo- and endonucleolytic activities rely on the same active site that is located at motif II of the metallo-β-lactamase domain. Together, these results demonstrated that *At*RNase J is active both as a robust endo-, as well as 5′→3′ exonuclease. In this sense, it differs from
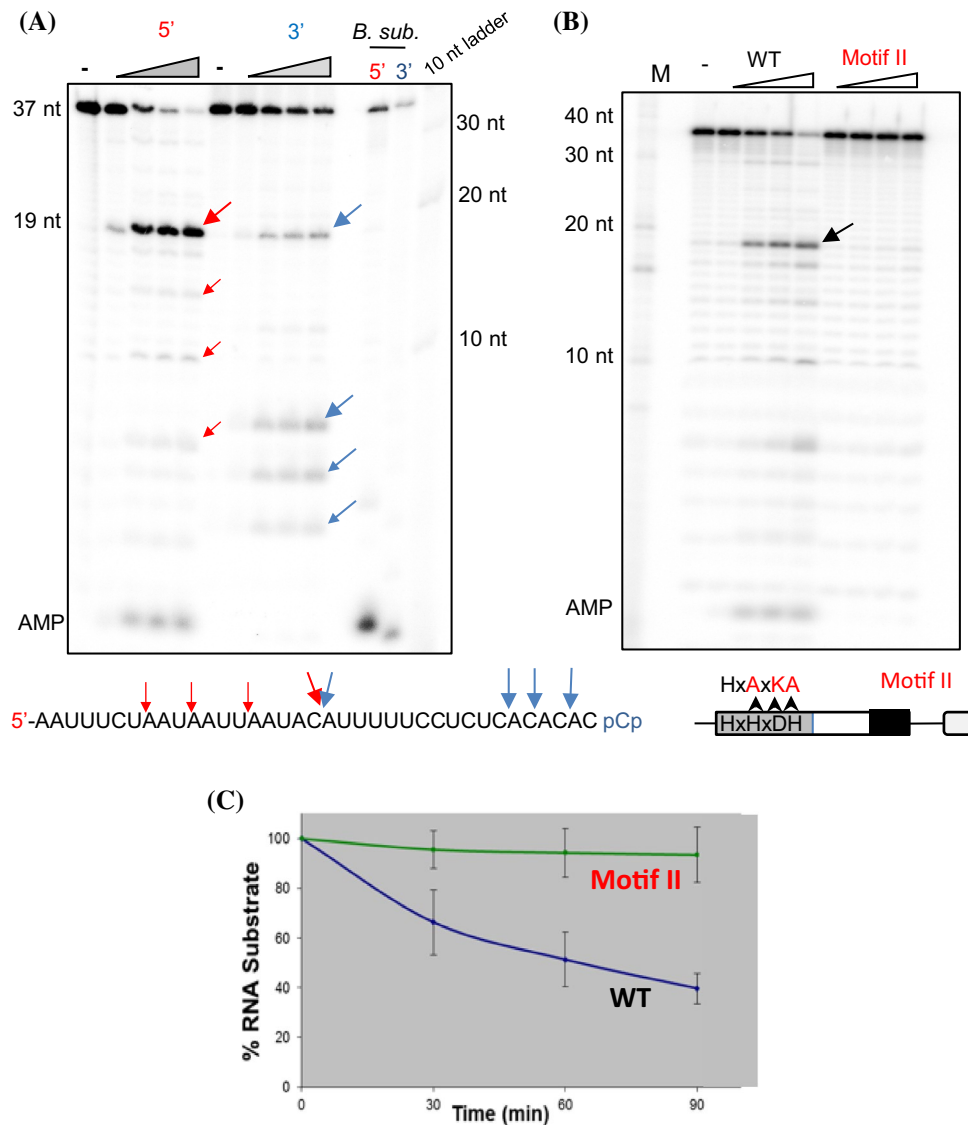
Fig. 2 *At*RNase J displays robust endonucleolytic as well as relatively weak exonucleolytic activities and mutating the conserved amino-acids of motif II eliminates both activities. **a** Recombinant *At*RNase J was incubated with a 5′ or 3′ end-^{32}P-labeled 37 nt RNA for 2, 30, 60 or 90 min, at 25 °C. For comparison, the same RNA was incubated with *B. subtilis* RNase J1 for 90 min (*B. sub.*). In the lane marked (-), RNA was incubated 90 min with no protein. Lane M—10 nt RNA marker. The nucleotide sequence of the substrate is shown at the bottom, with red arrowheads marking the 3′ ends of 5′-labeled endonucleolytic cleavage products. Blue arrowheads mark the 5′ ends of 3′-labeled cleavage products. Accumulation of ^{32}P-AMP resulting from 5′→3′ exonucleolytic activity, is evident with the 5′-labeled substrate. **b** The same 5′-labeled 37 nt RNA as used in **a** was incubated with wild-type *At*RNase J, or a mutated version where the three conserved amino acids of motif II were changed (Motif II). The three amino acids of motif II that were mutated are indicated at the bottom in red. **c** Quantification of the remaining full length 37 nt RNA in the reaction time points of experiments analyzing the activity of the Motif II as compared to the non-mutated protein (WT). Standard deviation bars were calculated using three independent experiments

the *Chlamydomonas* chloroplast RNase J which has been recently shown to harbor exclusively endoribonucleolytic activity when tested in vitro (Liponska et al. 2018). However, taken into account the robust endo- and relatively weak exonucleolytic activities, it is evident that the *At*RNase J is more similar to the *Chlamydomonas* enzyme than to the *B. subtilis* RNase J1.

Mutation of a single amino acid at the catalytic site (motif III) impaired the ribonucleolytic activity of *At*RNase J

Resolving the structures of bacterial and archaeal RNase Js revealed that the RNA is located to the active site as it is bound to a phosphate binding pocket that senses the amount of phosphates at the 5′ end on one side. On the other side

of the catalytic center, the RNA is hold in a "sandwiching" binding pocket [see Fig. 5 in Pei et al. (2015); Hausmann et al. (2017)]. In a search for mutants of *At*RNase J that the rate of degradation of the full length substrate is changed, we found that mutating Ser247 disclosed this incidence (Fig. 3). This conserved Serine (equivalent to Ser143, Ser152, Ser153 and Ser255 in *B. subtilis, C. coelicolor*, the archaea *M. psychrophilus* and the chloroplast of the green algae *C. reinhardtii* RNase J1 sequences, respectively), is part of motif III and forms hydrogen bond with a water molecule in the catalytic reaction center in adjustment to the two Zn ions, enabling the hydrolytic attack on the scissile phosphate (Pei

et al. 2015; Zheng et al. 2017). Replacing this Ser to Ala in the archaeal enzyme inhibited the exonucleolytic activity (Zheng et al. 2017). Here, it was replaced with Leu.

Upon incubation with the 5′-labeled 37 nt substrate, the S247L mutant enzyme proved significantly less degradation activity of the full length substrate, supporting the prediction that this conserved Ser of motif III is important for the activity (Fig. 3).

Therefore, and similar to what has been shown in archaea (Zheng et al. 2017), residue S247 contributes to the ribonuclease activity of the Arabidopsis enzyme. However, since the amount of accumulation of the intermediate degradation

Fig. 3 Mutating a single amino acid reduced the degradation activity of *At*RNase J while deletion of the GT-1 domain had no significant effect. **a** 5′-Labeled 37 nt RNA was incubated with wild-type *At*RNase J (WT) or a mutated protein in which serine 247 was changed to leucine (S247L, schematically shown at the bottom) for 2, 30, 60 and 90 min, at 25 °C. Controls included incubation of the RNA without protein (-) and with the *B. subtilis* RNase J1 (*B. sub.*), for 90 min. Lane M—10 nt RNA marker. **b** Same as in **a** analyzing the activity of a mutated *At*RNase J lacking the GT-1 domain (ΔGT-1). **c** and **d** Quantification of the remaining full length 37 nt RNA in the reaction time points of experiments analyzing the activity of the mutated proteins. Standard deviation bars were calculated using three independent experiments
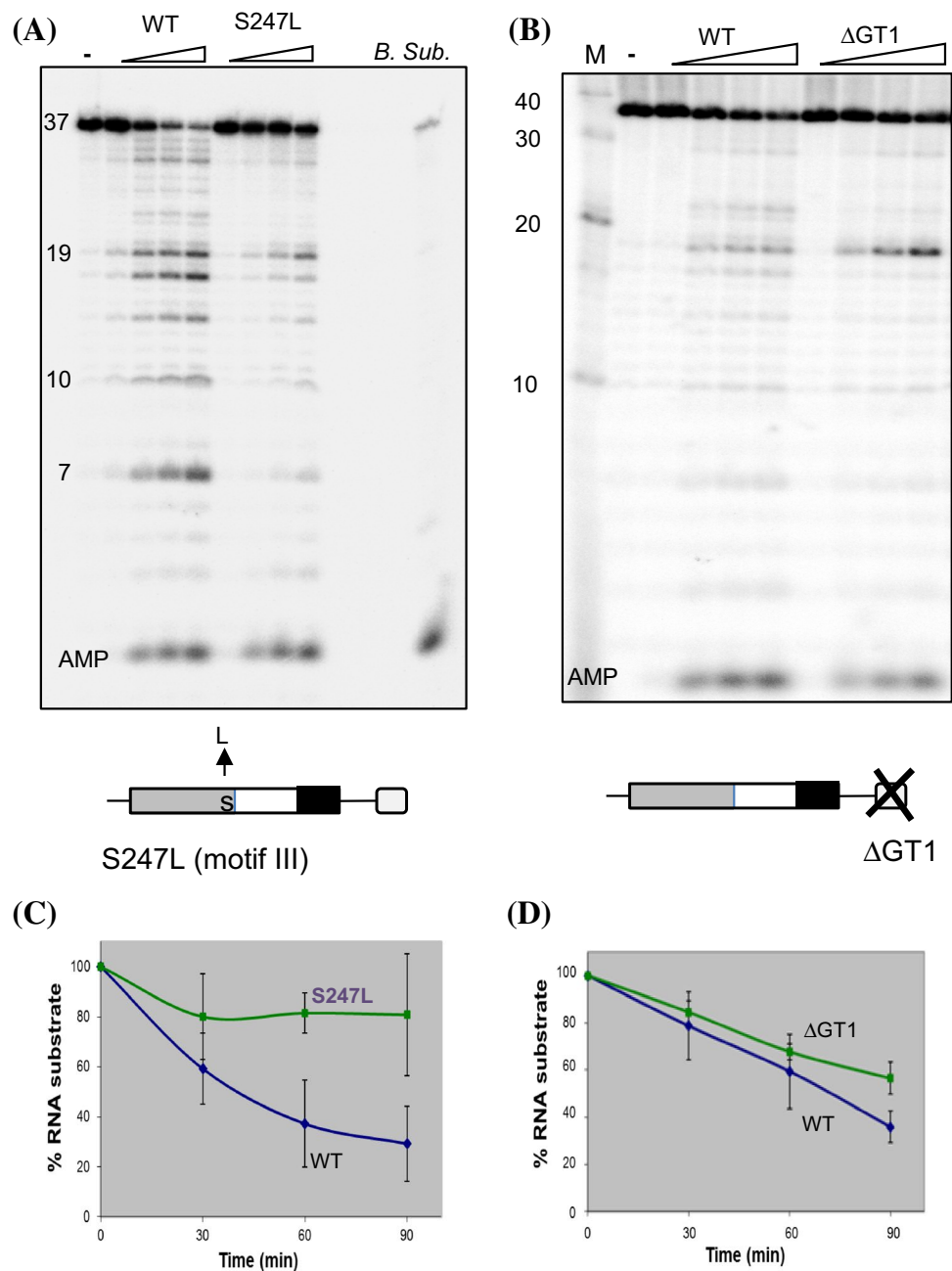
products were not highly reproducible in the several experiments analyzing this mutant, it was not possible at this stage to determine whether this residue is important for the exonucleolytic, the endonucleolytic or for both activities.

The plant-specific GT-1 domain is not essential for in vitro RNA degradation activity

The GT-1 domain was identified in transcription factors that specifically bind GT elements (5′-GGTTAA) that are present in light responsive promotors of nuclear encoded genes (Kaplan-Levy et al. 2012). The family of transcription factors consists of about 30 members in Arabidopsis and rice. Searching the protein sequence data bank using the *At*RNase J as a query, revealed homology between the carboxyl terminus of plant RNase J (amino acids 831–1010) and this domain (Figs. 1a, S1). The homology included three conserved tryptophan residues, each in one of the three helixes characteristic of the family, and the conserved sequence of a fourth helix that is present in most members of the family (Figs. S1, S2). The RNase J homologues of non-plant organisms lack the fragment showing homology to the GT-1 domain and, accordingly, are shorter (Fig. 1a). The C-terminal truncated *B. subtilis* RNase J1 protein is severely impaired in both exo- and endonucleolytic activities; further investigation of this truncated mutant revealed the role of this domain in maintaining its dimeric structure in solution (Mathy et al. 2007).

In order to analyze whether the GT-1 domain is important for the degradation activity of *At*RNase J, a truncated version, in which the GT-1 domain was deleted, was generated and analyzed for its rate of degradation of the full length substrate, as well as the endo- and exonucleolytic RNA-degradation activities (Fig. 3). Although slightly reduced activity was recorded and small differences in the accumulation of the cleavage products are observed in the experiment presented, these were not significant and reproducible in the several biological repeats of this analysis (Fig. 3). In general, there were not significant differences between the degradation activities of the WT and ΔGT-1 mutant in the rate of degrading the full length substrate, and both exo- and endonucleolytic activities were detected. Therefore, the GT-1 domain, which is unique to plants RNase J proteins, is not required for the exo- and endonucleolytic RNA degradation activities when analyzed in vitro with the tested 37 nt RNA. Further research is needed to determine the function of this evolutionarily added domain to the proper function of plant chloroplast RNase J proteins.

The nucleotide sequence of the substrate determines the exo- and endonucleolytic activities of *At*RNase J

To further study the mode of regulation of the 5′→3′ exo- and endonucleolytic activities of *At*RNase J, we analyzed the effect of the addition of three guanosines at the 5′ end of the RNA. Upon incubation of the recombinant *At*RNase J with 37 nt RNA bearing three guanosines at the 5′ end, both the exo- and endonucleolytic activities were significantly inhibited (< 15% degradation) as compared to the original substrate RNA (~ 70% degradation) (Fig. 4a).

The major endo- cleavage of the 37 nt substrate occurred between nucleotides C and A located at positions 19 and 20, respectively (Figs. 2, 3, 4). The same RNA labeled at the 3′ displayed three cleavages at other CA repeats (Fig. 2a). This raised the question whether the endo- cleavage is preferably directed to CA repeats. When replacing the dinucleotide CA at position 19–20 of the 37 nt RNA substrate with UG, the 19 nt cleavage product was not generated, while the exonucleolytic activity remained unchanged (Fig. 4b). Therefore, by changing the sequence of two nucleotides, the degradation activity of *At*RNase J shifted from being predominantly endo- to mostly an exonucleolytic. When assessing its activity on a 20 nt RNA substrate rich in guanosines and lacking the CA sequence, only limited and weak enzyme activity, which was mainly exonucleolytic, was observed (Fig. 5).

AtRNase J degrades single-stranded DNA and RNA better than double-stranded RNA

The bacterial RNase J1 of *Bacillus subtilis* was reported to cleave only single-stranded RNA (ssRNA), and this phenomenon has been exploited to monitor the secondary structure of RNA molecules (Daou-Chabo and Condon 2009). To determine whether *At*RNase J cleaves double-stranded RNA (dsRNA), 46, 31 and 15 nt substrates were generated. The 46 and 31 nt substrates form stem-loop structures while the 15 nt substrate formed just the ssRNA stem of the 31 nt substrate (Fig. 6 bottom). Upon incubation with *At*RNase J, several cleavages located mainly in the loops and the ssRNA tails of the substrates were observed (Fig. 6a). For example, the three dominant cleavages that characterized the ssRNA 15 nt substrate, were less pronounced in the 31 nt substrate, in which this same sequence is in the form of dsRNA. The major cleavage site of the 31 nt substrate was located at the loop of its stem-loop RNA. Similarly, for the 46 nt substrate, mostly cleavages at the ssRNA tails and the loop were obtained (Fig. 6a). Interestingly, the 5′ end nucleotide is not detected with these substrates indicating that these are poor substrates of the exonucleolytic activity. These results resembles those obtained in the in vivo analysis where cleavages in chloroplast transcripts of tobacco leaves that are related to RNase J were mapped (Luro et al. 2013). Taken together, similar to *Bacillus* RNase J1, *At*RNase J primarily cleaves ssRNA.

When *At*RNase J was presented with single-strand DNA (ssDNA) substrates, degradation was clearly observed (Fig. 6b). Activity of ssDNA degradation has been reported
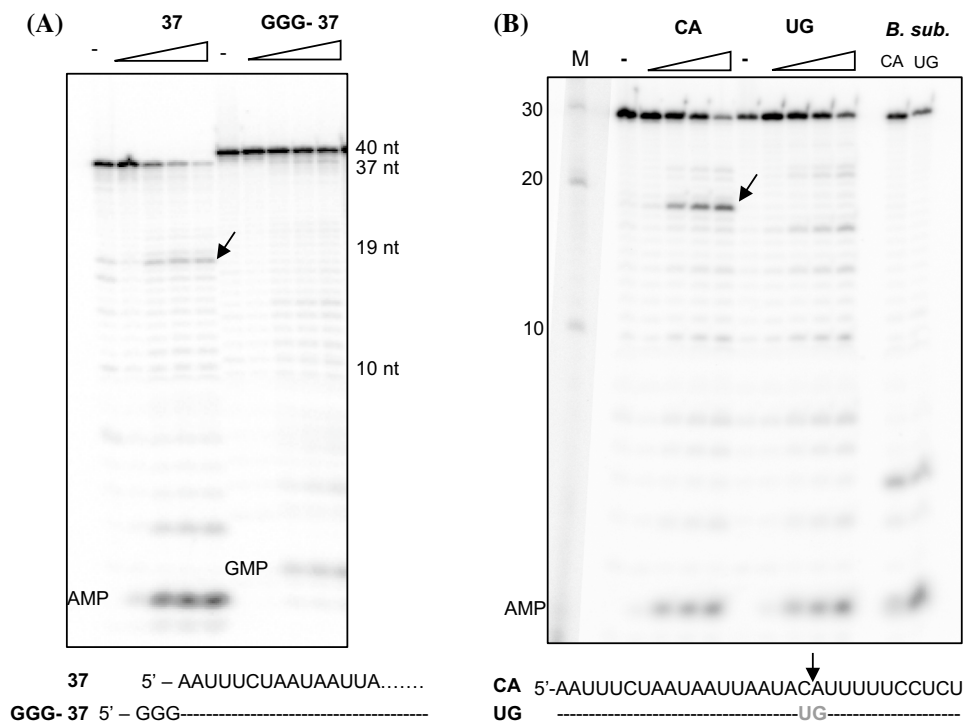
Fig. 4 Addition of three Gs at the 5′ of the substrate RNA significantly inhibited degradation while changing two nucleotides at the major endonucleolytic cleavage site eliminates the cleavage. **a** A 5′-labeled, 37-nt, A-U-rich RNA substrate, without or with the addition of three Gs at the 5′ end, as shown at the bottom, was incubated with *At*RNase J for 2, 15, 30 and 60 min, at 25 °C. Controls included incubation with no added *At*RNase J for 60 min (-). **b** 5′-labeled, 30-nt RNAs, harboring the CA (CA) or UG (UG) nucleotides at positions 18–19, were incubated with *At*RNase J for 2, 15, 30 or 60 min, at 25 °C. Controls included incubation without *At*RNase J (-) or with the *Bacillus* RNase J (*B. sub.*) for 60 min. Lane M—10 nt RNA ladder. Arrowhead indicates the 19-nt endo- cleavage product obtained with the CA substrate. [^{32}P]-AMP accumulation at the bottom of the gel indicates the 5′ to 3′ exonucleolytic activity

before for RNase Js of the extremophiles *Deinococcus radiodurans* (Zhao et al. 2015), *Methanocaldococcus jannaschii* (Levy et al. 2011) and *Methanolobus psychrophilus* (Zheng et al. 2017). Together, these results imply that *At*RNase J activity is modulated by the nucleotide sequence, and by the structure of the RNA substrate. This enzyme primarily cleaves ssRNA but can also degrade ssDNA.

Discussion

The unique feature of defining the ends of transcripts in plants chloroplast were uncovered in the last decay. In the absence of efficient transcription termination, a group of many specific nuclear-encoded RNA-binding proteins evolved. These proteins go into the chloroplasts and bind specific RNA sequences at the 3′ and 5′ UTRs, as well as the intergenic regions of multicistronic transcripts. Then, a ribonucleolytic digestion shorten the precursor transcript until it is blocked by the barrier formed by the protein bound to the RNA (Stern et al. 2010; Barkan 2011; Prikryl et al. 2011; Hammani et al. 2012; Zhelyazkova et al. 2012; Luro et al. 2013; Barkan and Small 2014; Manavski et al. 2018). In the

process of the generation of the mature 5′ end, RNase J is hypothesized to be the corresponding ribonuclease. Here, we characterized the in vitro activities of Arabidopsis chloroplast RNase J. We showed that recombinant *At*RNase J, produced in yeast cells and extensively purified to homogeneity, displays 5′→3′ exonucleolytic activity on ssRNA and ssDNA. In addition, this enzyme demonstrates robust endonucleolytic activity on ssRNA, which was modulated by the sequence of nucleotides and by the structure of the RNA substrate.

Expression and purification of *At*RNase J

*At*RNase J was found to be very difficult to express and purify in large quantities and devoid of any contaminating bacterial ribonucleases. When expressed in *E. coli*, the protein tends to form inclusion bodies even at low concentrations and to complex with PNPase and RNase E during several purification steps. We have previously overcome these difficulties by expressing the enzyme in a PNPase-deficient strain and performing many biochemical purification steps (Sharwood et al. 2011). Alternatively, a codon-optimized version of the gene was used for the *Chlamydomonas* enzyme (Liponska et al. 2018). In this work, we chose to use the yeast expression
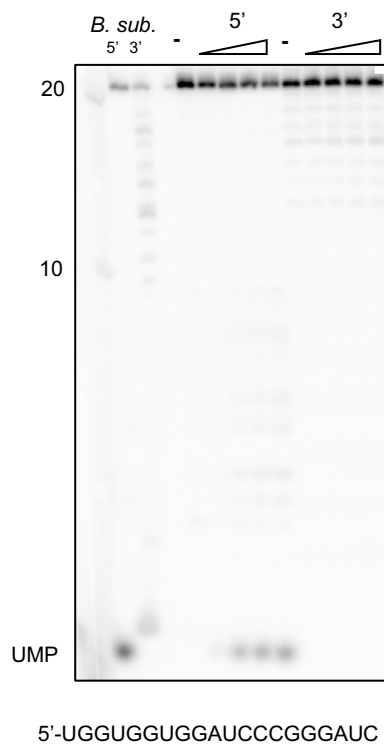
Fig. 5 Limited activity of *AtRNase J* degrading G rich RNA substrate. 5′ or 3′ labeled 20 nt G rich RNA substrate, as shown at the bottom, was incubated with the *At*RNase J for 2, 15, 30 and 60 min at 25°. Controls included incubation with no added protein (-) or with the *Bacillus* RNase J (*B. Sub.*), for 60 min. The accumulation of [^{32}P]-UMP as the result of the 5′ to 3′ exo- activity is evident at the bottom. The nucleotide sequence of the RNA substrate is shown at the bottom

system, which lacks PNPase and RNase E and produced a large amount of soluble protein which was rapidly purified in large quantities, without undergoing degradation. Yet, it was important to verify that none of the observed exo- and endonucleolytic activities that were characterized here resulted from an unidentified contaminant of the recombinant *At*RNase J with yeast proteins. Therefore, it was extremely important to generate the Motif II mutated version which lacks both exo- and endonucleolytic activities. Only after demonstrating that *At*RNase J was not contaminated with any unrelated ribonucleases, did we conclude that *At*RNase J harbors both 5′→3′ exonucleolytic and robust endonucleolytic activities.

Is the difference between the mode of activities of Arabidopsis and *Chlamydomonas* RNase J proteins related to different 5′ end processing mechanisms of chloroplast transcripts between higher plants and green algae?

RNase J was initially identified and characterized in bacteria as the only prokaryotic exonuclease that digests RNA

in the 5′→3′ direction (Mathy et al. 2007). Homologs that form a group of metallo-β-lactamase ribonucleases were identified in all other kingdoms of life (Condon and Gilet 2011; Dominski et al. 2013; Phung et al. 2013; Clouet-d'Orval et al. 2018). Similar to their evolutionary ancestor, cyanobacteria, the chloroplasts of higher plants contain both endoribonucleases RNase J and RNase E, in addition to the 3′→5′ exonucleases PNPase and RNase II/R, as well as other RNA metabolizing enzymes of prokaryotic origin. Interestingly, the green algae *Chlamydomonas reinhardtii* does not have a gene encoding RNase E/G but does contain a chloroplast RNase J (Liponska et al. 2018). Another striking difference is that while the 5′ and 3′ ends of chloroplast transcripts in higher plants are mostly defined by the binding of PPR or related RNA-binding proteins, there are only few PPR proteins in *Chlamydomonas* (Barkan and Small 2014). Yet, similar to plants, nuclear-encoded proteins bind the transcript untranslated regions and modulate expression in *Chlamydomonas* (Manavski et al. 2018). In addition, PPR proteins were also described to bind the untranslated regions of mitochondrial transcripts in plants, where the nature of the ribonuclease involved is yet to be identified (Hauler et al. 2013; Ruwe et al. 2016). It was recently reported that *Chlamydomonas* RNase J lacks 5′→3′ exonuclease activity in vitro, and various attempts to produce an exonucleolytically active recombinant enzyme were unsuccessful (Liponska et al. 2018). It remains unclear why the Arabidopsis enzyme displays both the exo- and endonucleolytic activities while that of *Chlamydomonas* displays exclusively endonucleolytic activity. One possibility is that there is a difference between the activities in vitro or in bacteria to that in the enzyme natural milieu in the chloroplast. Indeed, evidences of *Chlamydomonas* 5′→3′ exonucleolytic activity on chloroplast transcripts have been described before in experiments preformed in vivo (Drager et al. 1998, 1999). This activity could be performed by *Chlamydomonas* RNase J, if it is active as an exonuclease under in vivo conditions, or by a yet to be discovered enzyme that does not display homology to a bacterial enzyme. Another possibility is that the 5′→3′ exonucleolytic activity is required for the coordinated action of *At*RNase J with the specific RNA-binding proteins in the generation of the correct 5′ end of the transcript, while in *Chlamydomonas* the exonucleolytic activity is not required.

What is the function of the GT-1 domain in plant RNase J?

GT proteins belongs to the trihelix transcription factors family that is limited to plants and bind GT elements in genes regulated by light, biotic and abiotic stresses (Kaplan-Levy et al. 2012). The large family consists of

Fig. 6 *AtRNase* J degrades single stranded RNA and DNA. **a** 5′-Labeled 46, 31 and 15-nt RNA substrates forming stem-loops and ssRNA structures, as shown at the bottom of the figure, were incubated with *At*RNase J for 2, 15, 30 or 60 min. The lengths of the cleavage products were determined using the 10-nt size marker (Lane M) and RNA ladder (Lane L) shown to the right, and are presented in the sequences shown at the bottom using red, green and black colors for the 46, 31 and 15-nt substrates, respectively. Note that all cleavages were primarily in the loops and the ssRNA regions. **b** 5′-Labeled oligodeoxynucleotides of 57 nt (T7-37) and 50 nt (GAPDH) substrates were incubated with *At*RNase J for 0, 15, 30, 60 or 90 min, purified and then analyzed by denaturing urea-PAGE and autoradiography. A 10-nt size marker and RNA ladder were fractionated on the same gel (Lanes M and L). A kinetic demonstration of the degradation of the full-length substrates is presented in Fig. S3 of the supplemental data
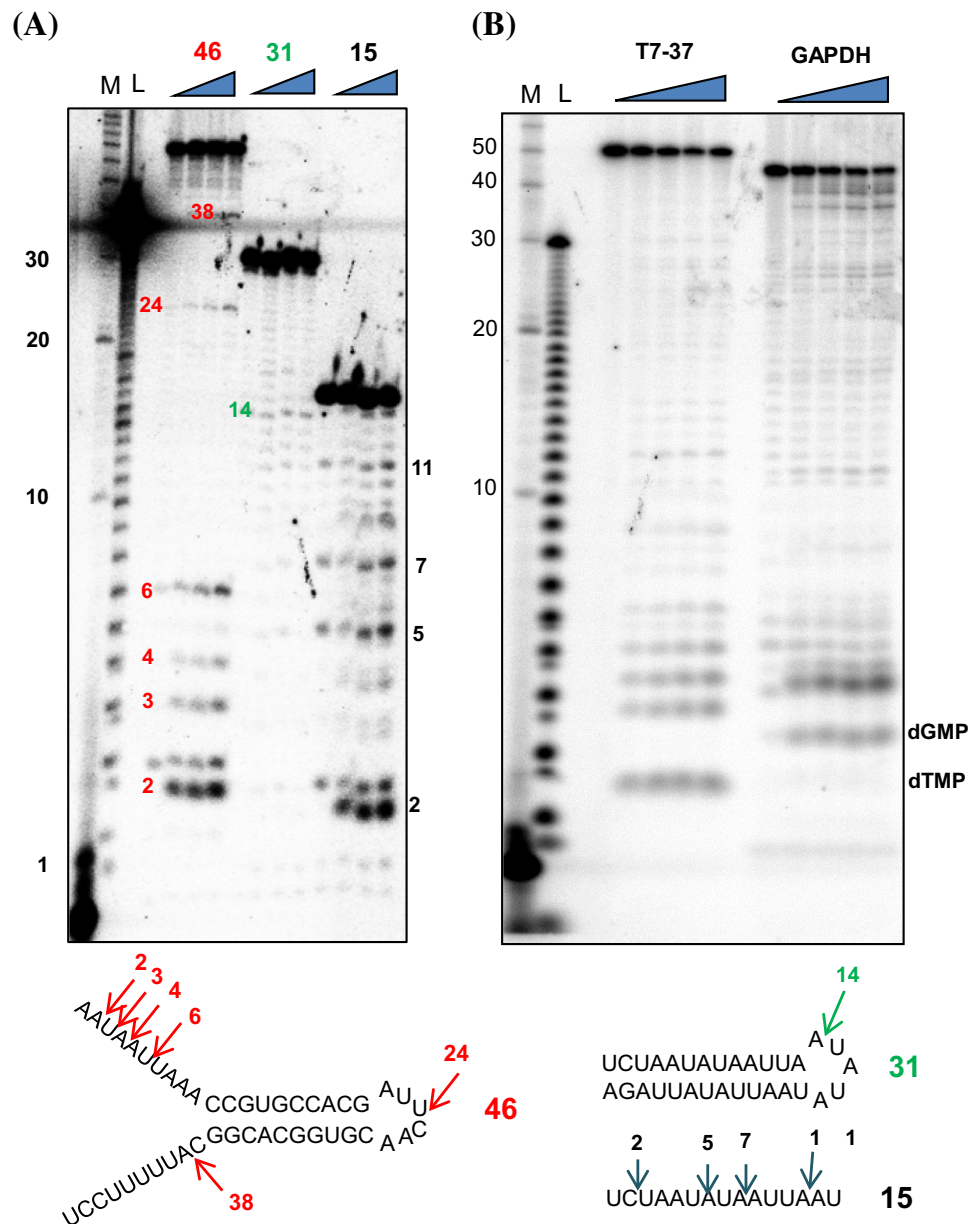
30, 31, 52 and 56 members in Arabidopsis, rice, *Brassica rapa* and *Populus trichocarpa*, respectively (Kaplan-Levy et al. 2012; Qin et al. 2014; Wang et al. 2016, 2017). GT-1 belongs to the GT-1 clade of five clades including in the trihelix transcription factors family. Structural analysis revealed three α-helical sequences separated by loop and turns where each helix contains a conserved tryptophan. An additional fourth amphipathic α-helices with conserved sequence is present in some of the GT-1 proteins and also in the GT-1 domain of plants RNase J. The GT-1 transcription factors are located in the nucleus, bind as dimers or tetramers GT sequences motives in the promotors of regulated genes. For some of them, DNA-binding is modulated by phosphorylation of threonine 133, which however is not conserved in the *At*RNase J (Fig. S1). Considering the evolution of MBL ribonucleases, present in all kingdoms of life without the addition of the GT-1 domain, and the addition of GT-1 domain found in all plants, the favored scenario is that the GT-1 domain was added to the RNase J at the early stage of the plant evolution.

What could be the function of this domain, which is characterized in transcription factors located in the nucleus, when present in the ribonuclease RNase J that is located in the chloroplast? One possibility is that it functions in DNA binding, localizing the enzyme to certain places along the chloroplast genome. Indeed, the high conservation of amino acids sequence forming the three α-helixes and the fourth amphipathic one in the plants RNase J, support the function

in DNA binding (Kaplan-Levy et al. 2012). Alternatively, the GT-1 domain may function in the chloroplast in RNA-binding, either single or double-stranded, adding additional control level to the ribonucleolytic activity.

How is RNase J involved in the processing of chloroplast transcripts?

Chloroplast transcription produces many multi- and several monocistronic transcripts that are further processed by splicing, editing, nucleotide modifications and transcript end maturation. The 5′ and 3′ ends are defined by specific RNA-binding proteins, mostly of the PPR family (Stern et al. 2010; Barkan and Small 2014). Accordingly, it has been proposed that RNase J digests the mRNA from its 5′ end until its activity is blocked by the specific RNA-binding protein bound to its binding site at the 5′ untranslated region of the transcript (Barkan 2011; Prikryl et al. 2011; Ruwe and Schmitz-Linneweber 2012; Zhelyazkova et al. 2012; Luro et al. 2013). Indeed, in experiments where PPR-bound RNAs were digested in vitro with an artificial and not of chloroplast origin 5′→3′ exoribonuclease, the digestion was inhibited when the exoribonuclease reached the PPR–RNA complex (Prikryl et al. 2011; Zhelyazkova et al. 2012). Obviously, the plant chloroplast RNase J is the apparent candidate to drive this activity. Therefore, the in vitro conditions used here may not precisely mimic the in vivo conditions. More studies using both in vivo and in vitro approaches will be necessary to uncover how RNase J, with its robust endonucleolytic activity, is involved in the generation of the 5′ ends of the chloroplast transcripts. One possibility is that RNA-binding proteins may direct endonucleolytic cleavages followed by exonucleolytic trimming until reaching the protein–RNA barrier complex. Possible regulatory aspects of the enzyme by RNA-binding proteins include RNA conformational changes upon protein binding, cleavage site exposure, and possible directing the ribonuclease cleavage activity through protein–protein interactions between RNase J, the gene specific RNA-binding protein such as a PPR one, and/or another protein yet to be identified. Null mutants of *At*RNase J are embryonic lethal with no development of mature chloroplasts that could be attributed to the inability to process the transcripts 5′ end and therefore hindering translation of chloroplast encoded proteins (Tzafrir et al. 2004; Chen et al. 2015). In addition, additional functions of *At*RNase J were observed when it was down expressed in tobacco leaves by virus induced gene silencing (VIGS) (Sharwood et al. 2011). Under this condition there was large accumulation of antisense transcripts in the chloroplast that were interacting with the sense transcripts prevent the translation of chloroplast encoded genes. How RNase J selectively digest antisense transcripts is yet to be revealed. Our results suggest that the specific elimination of antisense transcript could be related to its dual exo- and endonucleolytic activity.

Materials and methods

Cloning and expression of *AtRNase J*

Arabidopsis RNase J cDNA (At5g63420) was cloned, without the predicted chloroplast transit peptide, into the *Eco*RI and *Not*I restriction sites of the *Pichia pastoris* expression vector pPICZ (Invitrogen), which was then transformed into KM71H *Pichia* cells by electroporation, as described by the manufacture (Invitrogen). In order to find multi-copy recombinants, the colonies were grown on plates containing 1 or 2 mg/ml zeocin and the largest colonies were analyzed for recombinant protein expression. Colonies displaying the highest expression of the recombinant protein were grown overnight in BMGY medium (1% yeast extract, 2% peptone, 100 mM potassium phosphate pH 5.8, 1.34% YNB (without amino acids), 1% glycerol) at 28 °C, harvested and resuspended in BMMY medium (same as BMGY but replacing the glycerol with 0.5% methanol) and grown to $OD_{600} = 1.0$. The cells were further grown for 4 days at 23 °C, with the addition of 1% methanol every 24 h.

Purification of *Arabidopsis* RNase J

To purify the recombinant protein, the *Pichia* cell pellet was resuspended in lysis buffer containing 50 mM NaH_2PO_4 pH 7.0, 300 mM NaCl, 10% glycerol, 0.1% Triton X100, 10 mM imidazole, 2 mM DTT and protease inhibitor cocktail (Sigma). Cells were disrupted using a microfluidizer operating for six cycles at the highest pressure. The soluble fraction was applied to a cobalt talon resin, according to the manufacturer's instructions (Clontech). The elution fractions were loaded onto a 1 ml HiTrap heparin column (GE Healthcare) and eluted at a salt concentration of 0.84 M NaCl. The fractions were concentrated using 10,000 Da cutoff centricon (Sartotius) and loaded onto a Superdex 200 size-exclusion column (GE Healthcare) in the activity buffer (20 mM HEPES (pH 8.0), 300 mM NaCl, 8 mM $MgCl_2$, 5% glycerol and 2 mM DTT). The peak fractions were identified by immunoblot using either anti-His tag antibodies (Genscript) or anti-*At*RNase J antibodies prepared in our lab, deep-frozen in aliquots and stored at − 80 °C.

Expression and purification of *B. subtilis* RNase J

Escherichia coli BL21 Codon^{+} cells transformed with the expression vector pet28-YkqcHis containing the *B. subtilis* RNase J gene (Q45493) with a 6xHis tag at the C- terminus were kindly obtained from Ciaran Condon's lab (Mathy et al.

2007). The expression and purification of this protein were performed as described in (Mathy et al. 2007).

Site-directed mutagenesis

Site-directed mutagenesis was performed on the expression plasmid containing the *At*RNase J cDNA with the primers indicted in Table S2. Following PCR amplification with PFU polymerase (Thermo Scientific), the reaction mixture was incubated for 2 h with Dpn I (NEB), and transformed to DH5α competent cells.

Synthetic RNA synthesis for the in vitro assays

5′-end labeling of the short synthetic RNA was performed with T4 polynucleotide kinase and [γ-^{32}P]ATP, yielding 5′ mono-phosphorylated [^{32}P] substrates (Levy et al. 2016). 3′-end labeling of the RNA substrates were generated with T4 ligase and ^{32}[P]CTP, yielding a [^{32}P]-labeled RNA containing an additional C at the 3′ end (Levy et al. 2016). [^{32}P]-labeled RNAs where resolved on 15% denaturing polyacrylamide gels and the full length products were eluted from the gel by overnight incubation at 4 °C.

In vitro RNA degradation assays

In vitro RNA degradation assays were performed using the recombinant protein and either 5′ [^{32}P]-labeled or 3′ [^{32}P] CTP-labeled RNA substrates. Protein (10 μM) was incubated at 25 °C with 0.1–1.0 μM RNA for the times indicated in the figure legends. Following incubation, the RNA was analyzed by denaturing PAGE, followed by autoradiography (Levy et al. 2016). The length of the cleavage products was determined by running RNA length markers and alkaline ladder on the same gel. In several instances, the autoradiographs were overexposed in such a way that each length could be observed and use to determine the RNA length. The reported degradation rate is the average rate of disappearance of the full length substrate, measured in at least three independent experiments.

Author contributions MH—designed and performed the experiments. VL—designed and performed some of the experiments. FG—performed the bioinformatics analysis of the GT-1 domain. GS—designed the research, secured funding and wrote the manuscript.

References

Barkan A (2011) Update on expression of plastid genes expression of plastid genes: organelle-specific elaborations on a prokaryotic scaffold. Plant Physiol 155:1520–1532. https://doi.org/10.1104/pp.110.171231

Barkan A, Small I (2014) Pentatricopeptide repeat proteins in plants. Annu Rev Plant Biol 65:415–442. https://doi.org/10.1146/annurev-arplant-050213-040159

Chen H, Zou W, Zhao J (2015) Ribonuclease J is required for chloroplast and embryo development in Arabidopsis. J Exp Bot 66:2079–2091. https://doi.org/10.1093/jxb/erv010

Cho H-S, Byun J-S, Jun S-H (2008) Complex structure of plant telomere binding protein, NgTRF and telomere DNA. RCSB PDB. https://doi.org/10.2210/pdb2QHB/pdb

Clouet-d'Orval B, Batista M, Bouvier M, Quentin Y, Fichant G, Marchfelder A, Maier L-K (2018) Insights into RNA processing pathways and associated-RNA degrading enzymes in Archaea. FEMS Microbiol Rev 42:1–35. https://doi.org/10.1093/femsre/fuy016

Condon C, Gilet L (2011) Chap. 10: the metallo-beta-lactamase family of ribonucleases. In: Nicholson AW (ed) Ribonucleases, nucleic acids and molecular biology. Springer, Berlin, pp 245–267

Daou-Chabo R, Condon C (2009) RNase J1 endonuclease activity as a probe of RNA secondary structure. RNA 15:1417–1425. https://doi.org/10.1261/rna.1574309

De La Sierra-Gallay IL, Zig L, Jamalli A, Putzer H (2008) Structural insights into the dual activity of RNase. J Nat Struct Mol Biol 15:206–212. https://doi.org/10.1038/nsmb.1376

Dominski Z (2007) Nucleases of the metallo-beta-lactamase family and their role in DNA and RNA metabolism. Crit Rev Biochem Mol Biol 42:67–93. https://doi.org/10.1080/10409230701279118

Dominski Z, Carpousis AJ, Clouet-d'Orval B (2013) Emergence of the beta-CASP ribonucleases: highly conserved and ubiquitous metallo-enzymes involved in messenger RNA maturation and degradation. Biochim Biophys Acta 1829:532–551. https://doi.org/10.1016/j.bbagrm.2013.01.010

Dorleans A, Li de la Sierra-Gallay I, Piton J, Zig L, Gilet L, Putzer H, Condon C (2011) Molecular basis for the recognition and cleavage of RNA by the bifunctional 5′-3′ exo/endoribonuclease RNase. J Structure 19:1252–1261. https://doi.org/10.1016/j.str.2011.06.018

Drager RG, Girard-Bascou J, Choquet Y, Kindle KL, Stern DB (1998) In vivo evidence for 5′→3′ exoribonuclease degradation of an unstable chloroplast mRNA. Plant J 13:85–96. https://doi.org/10.1046/j.1365-313X.1998.00016.x

Drager RG, Higgs DC, Kindle KL, Stern DB (1999) 5′ to 3′ exoribonucleolytic activity is a normal component of chloroplast mRNA decay pathways. Plant J 19:521–531. https://doi.org/10.1046/j.1365-313X.1999.00546.x

Even S, Pellegrini O, Zig L, Labas V, Vinh J, Brechemmier-Baey D, Putzer H (2005) Ribonucleases J1 and J2: two novel endoribonucleases in B.subtilis with functional homology to E.coli RNase E. Nucleic Acids Res 33:2141–2152. https://doi.org/10.1093/nar/gki505

Hammani K, Cook WB, Barkan A (2012) RNA binding and RNA remodeling activities of the half-a-tetratricopeptide (HAT) protein HCF107 underlie its effects on gene expression. Proc Natl Acad Sci USA 109:5651–5656. https://doi.org/10.1073/pnas.1200318109

Hauler A, Jonietz C, Stoll B, Stoll K, Braun HP, Binder S (2013) RNA processing factor 5 is required for efficient 5′ cleavage at a processing site conserved in RNAs of three different mitochondrial genes in Arabidopsis thaliana. Plant J 74:593–604. https://doi.org/10.1111/tpj.12143

Hausmann S. Guimarães S, Garcin VA, Baumann D, Linder N, Redder P (2017) Both exo- and endo-nucleolytic activities of RNase J1 from Staphylococcus aureus are manganese dependent and active on triphosphorylated 5′-ends. RNA Biol 14:1431–1443. https://doi.org/10.1080/15476286.2017.1300223

Kaplan-Levy RN, Brewer PB, Quon T, Smyth DR (2012) The trihelix family of transcription factors—light, stress and development. Trends Plant Sci 17:163–171. https://doi.org/10.1016/j.tplants.2011.12.002

Levy S, Portnoy V, Admon J, Schuster G (2011) Distinct activities of several RNase J proteins in methanogenic archaea. RNA Biol 8:1073–1083. https://doi.org/10.4161/rna.8.6.16604

Levy S, Allerston CK, Liveanu V, Habib MR, Gileadi O, Schuster G (2016) Identification of LACTB2, a metallo-beta-lactamase protein, as a human mitochondrial endoribonuclease. Nucleic Acids Res 44:1813–1832. https://doi.org/10.1093/nar/gkw050

Liponska A, Jamalli A, Kuras R, Suay L, Garbe E, André F, Laalami S, Putzer H (2018) Tracking the elusive 5 ′ exonuclease activity of Chlamydomonas reinhardtii RNase J. Plant Mol Biol 96:641–653. https://doi.org/10.1007/s11103-018-0720-2

Luro S, Germain A, Sharwood RE, Stern DB (2013) RNase J participates in a pentatricopeptide repeat protein-mediated 5′ end maturation of chloroplast mRNAs. Nucleic Acids Res 41:9141–9151. https://doi.org/10.1093/nar/gkt640

Manavski N, Schmid L-M, Org Meurer J, Meurer J (2018) RNA-stabilization factors in chloroplasts of vascular plants. Essays Biochem 62:51–64. https://doi.org/10.1042/EBC20170061

Mathy N, Benard L, Pellegrini O, Daou R, Wen T, Condon C (2007) 5′-to-3′ exoribonuclease activity in bacteria: role of RNase J1 in rRNA maturation and 5′ stability of mRNA. Cell 129:681–692. https://doi.org/10.1016/j.cell.2007.02.051

Meng EC, Pettersen EF, Couch GS, Huang CC, Ferrin TE (2006) Tools for integrated sequence-structure analysis with UCSF Chimera. BMC Bioinform 7:339–349. https://doi.org/10.1186/1471-2105-7-339

Nagano Y (2000) Several features of the GT-factor trihelix domain resemble those of the Myb DNA-binding domain. Plant Physiol 124:491–494. https://doi.org/10.1104/pp.124.2.491

Nagata T, Niyada E, Fujimoto N, Nagasaki Y, Noto K, Miyanoiri Y, Murata J, Hiratsuka K, Katahira M (2010) Solution structures of the trihelix DNA-binding domains of the wild-type and a phosphomimetic mutant of Arabidopsis GT-1: mechanism for an increase in DNA-binding affinity through phosphorylation. Proteins Struct Funct Bioinform 78:3033–3047. https://doi.org/10.1002/prot.22827

Pei XY, Bralley P, Jones GH, Luisi BF (2015) Linkage of catalysis and 5′ end recognition in ribonuclease RNase J. Nucleic Acids Res 43:8066–8076. https://doi.org/10.1093/nar/gkv732

Phung DK, Rinaldi D, Langendijk-Genevaux PS, Quentin Y, Carpousis AJ, Clouet-d′Orval B (2013) Archaeal beta-CASP ribonucleases of the aCPSF1 family are orthologs of the eukaryal CPSF-73 factor. Nucleic Acids Res 41:1091–1103. https://doi.org/10.1093/nar/gks1237

Prikryl J, Rojas M, Schuster G, Barkan A (2011) Mechanism of RNA stabilization and translational activation by a pentatricopeptide repeat protein. Proc Natl Acad Sci USA 108:415–420. https://doi.org/10.1073/pnas.1012076108

Qin Y, Ma X, Yu G, Wang QI, Wang L, Kong L, Kim W, Wang HW, Guanghui Y, Wang QI, Liang W, Kong L, Kim W, Wang HW (2014) Evolutionary history of trihelix family and their functional diversification. DNA Res 21:499–510. https://doi.org/10.1093/dnares/dsu016

Ruwe H, Schmitz-Linneweber C (2012) Short non-coding RNA fragments accumulating in chloroplasts: footprints of RNA binding proteins? Nucleic Acids Res 40:3106–3116. https://doi.org/10.1093/nar/gkr1138

Ruwe H, Wang G, Gusewski S, Schmitz-Linneweber C (2016) Systematic analysis of plant mitochondrial and chloroplast small RNAs suggests organelle-specific mRNA stabilization mechanisms. Nucleic Acids Res 44:7406–7417. https://doi.org/10.1093/nar/gkw466

Sharwood RE, Halpert M, Luro S, Schuster G, Stern DB (2011) Chloroplast RNase J compensates for inefficient transcription termination by removal of antisense RNA. RNA 17:2165–2176. https://doi.org/10.1261/rna.028043.111

Stern DB, Goldschmidt-Clermont M, Hanson MR (2010) Chloroplast RNA metabolism. Annu Rev Plant Biol 61:125–155. https://doi.org/10.1146/annurev-arplant-042809-112242

Tzafrir I, Pena-Muralla R, Dickerman A, Berg M, Rogers R, Hutchens S, Sweeney TC, McElver J, Aux G, Patton D, Meinke D (2004) Identification of genes required for embryo development in Arabidopsis. Plant Physiol 135:1206–1220. https://doi.org/10.1104/pp.104.045179

Wang Z, Liu Q, Wang H, Zhang H, Xu X, Li C, Yang C (2016) Comprehensive analysis of trihelix genes and their expression under biotic and abiotic stresses in Populus trichocarpa. Sci Rep 6:36274. https://doi.org/10.1038/srep36274

Wang W, Wu P, Liu T, Ren H, Li Y, Hou X (2017) Genome-wide analysis and expression divergence of the Trihelix family in *Brassica rapa*: insight into the evolutionary patterns in plants. Sci Rep 7:6463. https://doi.org/10.1038/s41598-017-06935-0

Zhao Y, Lu M, Zhang H, Hu J, Zhou C, Xu Q, Ul Hussain Shah AM, Xu H, Wang L, Hua Y (2015) Structural insights into catalysis and dimerization enhanced exonuclease activity of RNase J. Nucleic Acids Res 43:5550–5559. https://doi.org/10.1093/nar/gkv444

Zhelyazkova P, Hammani K, Rojas M, Voelker R, Vargas-Suárez M, Börner T, Barkan A (2012) Protein-mediated protection as the predominant mechanism for defining processed mRNA termini in land plant chloroplasts. Nucleic Acids Res 40:3092–3105. https://doi.org/10.1093/nar/gkr1137

Zheng X, Feng N, Li D, Dong X, Li J (2017) New molecular insights into an archaeal RNase J reveal a conserved processive exoribonucleolysis mechanism of the RNase J family. Mol Microbiol 106:351–366. https://doi.org/10.1111/mmi.13769